Corrosion Science 92 (2015) 309–314

Contents lists available at ScienceDirect

Corrosion Science

journal homepage: www.elsevier.com/locate/corsci

Short Communication

# The influence of vibration and probe movement on SVET measurements

A.C. Bastos [*], M.C. Quevedo, M.G.S. Ferreira

*CICECO/DEMaC, Universidade de Aveiro, 3810-193 Aveiro, Portugal*

A R T I C L E   I N F O

*Article history:*
Received 7 July 2014
Accepted 25 October 2014
Available online 1 November 2014

*Keywords:*
SVET
Scanning vibrating electrode technique

A B S T R A C T

This communication describes a set of experiments performed to evaluate the influence of SVET vibration and movement of the probe on the obtained results. Both vibration and movement during scanning stir the solution with the risk of enhancing the oxygen transport to the surface thus increasing the measured currents and accelerating the corrosion process. It is shown that, for the SVET system used, due to its small probe, the effect of the vibration is negligible in normal operation. On the contrary, the movement of the probe during scanning increases the cathodic reaction and smaller excursions or slower movements just marginally reduce this effect. It is also shown that only the region of the sample under the probe is affect and for just brief instants. The overall corrosion in the long run is not influenced and the measured maps only scarcely show any evidences of artifacts introduced by the probe movement.

## 1. Introduction

The scanning vibrating electrode technique (SVET) has been applied to characterise a great variety of corrosion systems [1–11]. The visualisation of the corrosion progression in terms of the identification of anodic and cathodic regions with estimation of the respective currents and their evolution in space and time is usually sufficient. However, it may be important to go further and use the SVET data for modelling purposes or to estimate corrosion rates. When such quantitative information is necessary, the experimental data must be absolutely accurate which means that all experimental parameters must be well known and controlled at all times. In addition, it is assumed that SVET does not interfere in any way with the system under study. Usually the sample corrodes freely at open circuit potential with the probe scanning above it without any contact between the two. The probe vibrates in order to generate the sinusoidal signal required for the amplification and filtering in a lock-in amplifier.

The effect of the probe vibration in biological systems was analysed by Ferrier and Lucas [12] who showed that the convective loops produced by the probe do not affect the electrical current density but can significantly change the ion concentration gradients in the layer near a tissue or cell surface and, sometimes, even the electrical potential gradient. In the corrosion context, McMurray et al. [13] analysed the influence of the probe vibration on the transport of $O_2$ to the metal surface. Using a 25 μm Pt disk polarised as cathode they identified the probe-to-sample distance and the amplitude of vibration as critical factors and observed that, in some conditions, the vibrating probe was able to increase the oxygen reduction current by a factor of 3–4. The effect of probe vibration on the corrosion of cut edges of galvanized steel, where oxygen diffusion to the metal surface is the rate determining step, was also studied in the same work. It was observed that while an increase in amplitude increased the local cathodic currents beneath the probe, the vibration did not affect the overall measured total anodic current because it did not significantly alter the rate of oxygen reduction across the entire sample. An overestimation of the total cathodic current by up to an order of magnitude resulted from large amplitude vibrations ~25–250 μm. An optimum small amplitude vibration <25 μm was considered critical to the quality of the data obtained using SVET.

Different SVET systems and probes exist that may affect the measurements and the corrosion process in different manners and extents. In the case of reference [13] the tip of the vibrating probe was a glass disk of 250 μm in diameter with a central active Pt disk of 125 μm diameter. Another model of SVET, used by many groups and by the authors of this work, employs a probe with a tip of usually 20 ± 10 μm and vibration amplitude of the same order of magnitude, being the measurements performed typically in a plane 50–200 μm above the sample surface.

It is important to check whether or not this SVET system suffers from the same reported problem and identify the parameters most relevant to it. For that purpose, in this work the SVET measured the ionic currents above a platinum disk polarised at potentials where oxygen reduction is controlled by diffusion, while the current in the circuit was being simultaneously measured. This permitted to assess the level of alteration introduced by the SVET scans.

---

[*] Corresponding author.
*E-mail address:* acbastos@ua.pt (A.C. Bastos).

http://dx.doi.org/10.1016/j.corsci.2014.10.038
0010-938X/

Another experiment made use of a Zn–Fe galvanic couple with the galvanic current being recorded while SVET maps were being acquired. In this way it was possible to observe how a typical corrosion system was affected by SVET in normal operation.

## 2. Experimental

The SVET equipment was manufactured by Applicable Electronics Inc. (USA) and controlled by the ASET 2.00 program developed by Sciencewares (USA). The SVET microelectrode was prepared from polymer insulated platinum–iridium microelectrodes produced by Microprobes Inc. (USA). A 20 µm diameter platinum black sphere was electrodeposited at the tip. The microelectrode vibrates in two directions, one parallel (*x* axis) and another normal (*z* axis) to the sample surface, sensing the electric field in the two directions, but in corrosion the signals for the *x* vibration are seldom used. The *x* and *z* frequencies were 115 Hz and 69 Hz, respectively, and the amplitude of both vibrations was 10 µm. After arriving to a new point of measurement the probe waited 0.2 s and averaged for more 0.2 s before moving to the next point. The SVET measures potential differences which are converted to current densities after a calibration performed with a point current source (microelectrode with a tip of ~2 µm) driving a current of 60 nA at 150 µm from the vibrating probe [14–16]. The calibration is valid for a new solution provided the system is updated with its conductivity.

The two electrochemical cells used are depicted in Fig. 1. The first consisted of 1 mm diameter platinum disk electrode embedded in epoxy matrix, connected to Ivium CompactStat potentiostat (Ivium Technologies, The Netherlands) in a 3 electrode arrangement with the platinum disk as working electrode, a platinum wire as counter electrode and a homemade Ag|AgCl|0.05 M NaCl electrode as reference. A second cell consisted of 1 mm pure zinc disk galvanically coupled to 1 mm pure iron disk. The galvanic current was measured with the Ivium Compactstat. The surfaces of both samples were abraded to SiC 4000 grade before experiments. In all cases the solution was 0.05 M NaCl at 23 ± 1 °C (conductivity = $5.18 \times 10^{-3}$ S cm$^{-1}$, at 23.0 °C).

## 3. Results and discussion

In the first experiment, the effect of SVET during scanning above a platinum disk where reduction reactions are taking place was analysed and the results are depicted in Fig. 2. Fig. 2(a) shows the current–potential curve of the platinum disk in 0.05 M NaCl at a scan rate of 1 mV s$^{-1}$ with the region of diffusion control between $-0.5$ $V_{Ag|AgCl}$ and $-0.9$ $V_{Ag|AgCl}$, and the region dominated by $H_2O$ reduction from $-0.9$ $V_{Ag|AgCl}$ to more negative potentials. The inset of Fig. 2(a) shows the chronoamperometric response of the electrode polarised at $-0.75$ $V_{Ag|AgCl}$. After a Cotrellian behaviour in the first ~3 min the current stabilised around 500 nA due to natural convection. The chronoamperometric measurement was repeated at different fixed potentials with SVET maps being acquired 100 µm above the surface. The chosen potentials were 0 $V_{Ag|AgCl}$, where almost no reaction occurs, $-0.5$ and $-0.75$ $V_{Ag|AgCl}$, in the region of diffusion control, and $-1$ $V_{Ag|AgCl}$, where $H_2O$ reduction is the predominant reaction. The SVET measurements started only after a stable reduction current was attained. Each map comprised 20 × 20 points and in Figs. 2(bx) they correspond to the interval 100–388 s of the chronoamperograms. The records of the current clearly display the influence of the SVET measurements in the form of periodic variations. These coincided with the passage of the probe above the Pt disk while scanning left–right and right-left, line after line. Each scan line produces a rise and a fall in the current, with the maximum being coincident with the middle of the disk. The movement of the probe enhances the transport of dissolved oxygen from the bulk of solution to the cathode increasing the reduction current. The process is fast, with a sudden increase when the probe enters the area above the cathode followed by a rapid decrease as soon as it moves away.

The highest current variations occurred during the first lines of the scan whereas in the last lines just small variations were observed. This is related to the position of the probe. The SVET probe is basically a ball shaped platinum microelectrode tip at the end of an insulated wire inclined over the surface (Fig. 1c). The maps are acquired with the tip going from top to the bottom of the image. In the first lines the tip is over the insulating matrix but the wire is above the Pt disk. This induces the largest convection and produces the maximum disturbance. As the scan progresses, less Pt area is under that “moving wire”. In the middle of the scan only half of the Pt disk is affected and in the last lines the probe is no longer above the disk and the effect vanishes.

The hydrodynamics induced by the probe is a subject to be investigated in future work.

Fig. 2(b2) compares the perturbation introduced by the probe when it scans at 100 µm with and without vibration and when it scans vibrating at 200 µm. The measurement performed at 200 µm had smaller impact on the current, leading to a maximum increase of 10% compared to 20% at 100 µm. The currents with the probe scanning at 100 µm with and without vibration were nearly the same, with a difference of only 15 nA. This means that it is the movement of the probe during scanning that creates most of the disturbance. The vibration just adds a limited contribution.

The effect is more important when the process is controlled by the diffusion of $O_2$ ($-0.5$ $V_{Ag|AgCl}$ and $-0.75$ $V_{Ag|AgCl}$). The relative

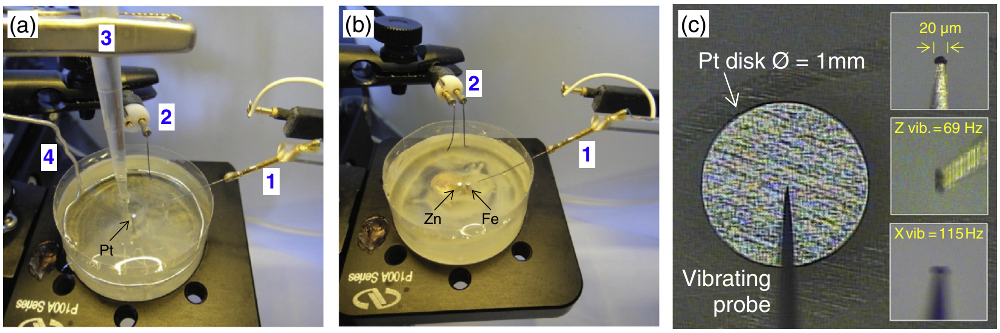

**Fig. 1.** Electrochemical cells used: externally polarised 1 mm diameter platinum disk (a) and galvanically coupled 1 mm diameter zinc and iron disks (b) where 1 – vibrating electrode, 2 – pseudo-reference electrode and ground (ground electrode removed in (a)), 3 – homemade Ag|AgCl reference electrode, 4 – platinum wire counter electrode. Also shown is the size, shape and vibration of the SVET probe (c).

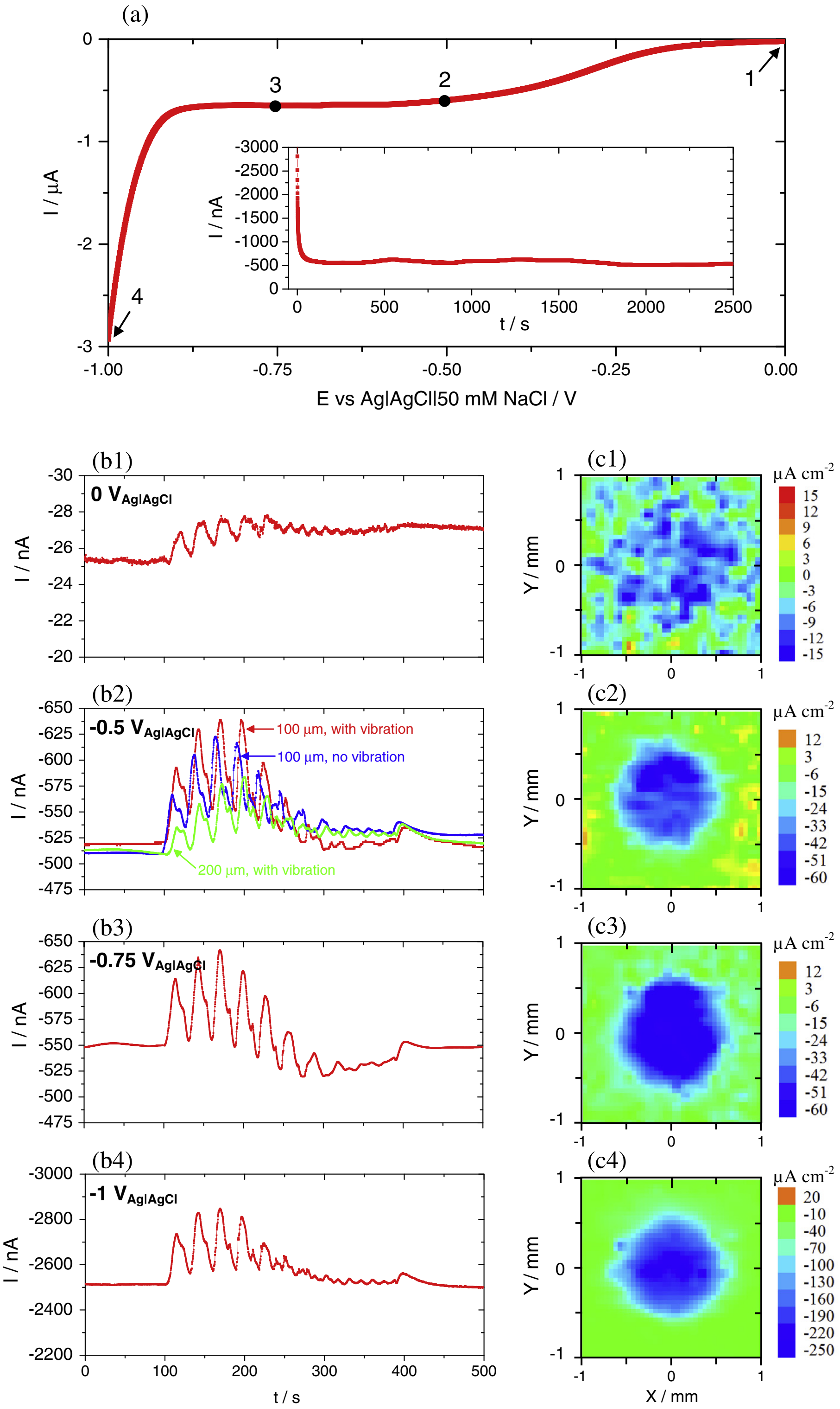

**Fig. 2.** Current–potential curve of 1 mm platinum disk in 0.05 M NaCl with the chronoamperometric response at $-0.75$ $V_{Ag|AgCl}$ as inset (a) and chronoamperometric curves (bx) and SVET maps (20 × 20 points) (cx) measured with the Pt disk polarised at 0 $V_{Ag|AgCl}$ ($x = 1$), $-0.5$ $V_{Ag|AgCl}$ ($x = 2$), $-0.75$ $V_{Ag|AgCl}$ ($x = 3$) and $-1$ $V_{Ag|AgCl}$ ($x = 4$).

current increase was not so high at 0 $V_{Ag|AgCl}$ and at $-1$ $V_{Ag|AgCl}$, potentials where the reductions of, respectively, dissolved $O_2$ and $H_2O$, were controlled by activation.

The SVET maps were measured 100 μm above the surface and exhibited a central region of negative current over the platinum surrounded by absence of current over the polymer matrix. These current densities correspond to the component normal to the surface ($i_z$) and were around $-50$ μA cm$^{-2}$ for polarisations of $-0.5$ $V_{Ag|AgCl}$ and $-0.75$ $V_{Ag|AgCl}$ and $-200$ μA cm$^{-2}$ for the polarisation of $-1$ $V_{Ag|AgCl}$. Taking the currents measured by the potentiostat it is possible to estimate the current density that should be measured by SVET 100 μm above a disk electrode with a diameter of 1 mm, considering two ideal cases: an equipotential disk and a uniform current disk. The equations are, respectively [17,18],

$$i = \frac{I}{2\pi(r^2 + z^2)} \tag{1}$$

$$i = \frac{I}{\pi r^2}\left(\frac{1}{r} - \frac{z}{r^2\sqrt{1+\frac{z^2}{r^2}}}\right) \tag{2}$$

where $i$ is the current density at a height $z$ exactly above the centre of the disk of radius $r$ for a current $I$ circulating in the circuit. Table 1 shows the calculated current densities for the cathodic limit currents in Fig. 2. In 3 out of 4, the values measured by SVET lied within the limits of Eqs. (1) and (2). It must be noted that these equations work for ideal and well behaved systems. For real samples reliable predictions are expected to be provided only by numerical modelling.

**Table 1**
Average current densities measured 100 μm above a Pt disk of 1 mm diameter driving a total current $I$ and values estimated considering an equipotential disk (Eq. (1)) and a uniform current disk (Eq. (2)).

| I/nA | i/μA cm$^{-2}$ | | |
|---|---|---|---|
| | SVET average value | Equipotential disk (Eq. (1)) | Uniform current disk (Eq. (2)) |
| 25 | 6 | 1.5 | 2.6 |
| 525 | 45 | 32 | 54 |
| 550 | 50 | 34 | 56 |
| 2500 | 200 | 153 | 256 |

The measurements in Fig. 2 pointed to a small contribution from the vibration. To confirm this small effect, the probe was placed in the centre of the disk with vibration on or off while the reduction current at the Pt disk was being recorded – Fig. 3. Minor changes in current were observed with the 10 μm amplitude. The variation was larger when the probe was closer to the surface but the most significant effect occurred when the vibration amplitude was increased. It should be remembered that distances closer than 50 μm and vibration amplitudes higher than 20 μm are hardly used. These results clearly confirm the small effect of vibration in typical conditions of operation.

After the experiments with the platinum electrode, similar tests were made with a system simulating a typical corrosion system. A Zn–Fe galvanic couple with the configuration shown in Fig. 1(b) was chosen because it gives a clear separation of the anode and the cathode and the possibility to measure the galvanic current, thus allowing a better characterisation of the effect of SVET. Fig. 4 shows galvanic currents and SVET maps measured in the same conditions as before and similar to the usual operation parameters used in corrosion studies. It is evident that the spatial resolution increases as the probe scans closer to the surface. The current distribution was essentially uniform at the cathode while at the anode it was more localised, as expected for the corrosion of zinc in near neutral chloride solutions [14,19]. The recordings of the galvanic current displayed periodic variations similar to the ones observed with the platinum cathode. The variations coincided with the passage of the probe above the iron disk (cathode) and no change was registered when it passed above the zinc. The reason is again the enhancement of transport of dissolved $O_2$ to the surface of the cathode through a convective effect induced by the movement of the probe. Fig. 4(b2) compared once more the effect of a scan with and without vibration and, again, the effect on current was similar, regardless the vibration being on or off.

The increase of the cathodic current takes place precisely when it is being measured. Therefore, an unbalance between anodic and cathodic currents measured by SVET can be expected and it, in fact, occurs, with the integration of the cathodic currents being 10–30% higher than the integrated anodic currents. It is to be noted that the mismatch between anodic and cathodic currents in SVET

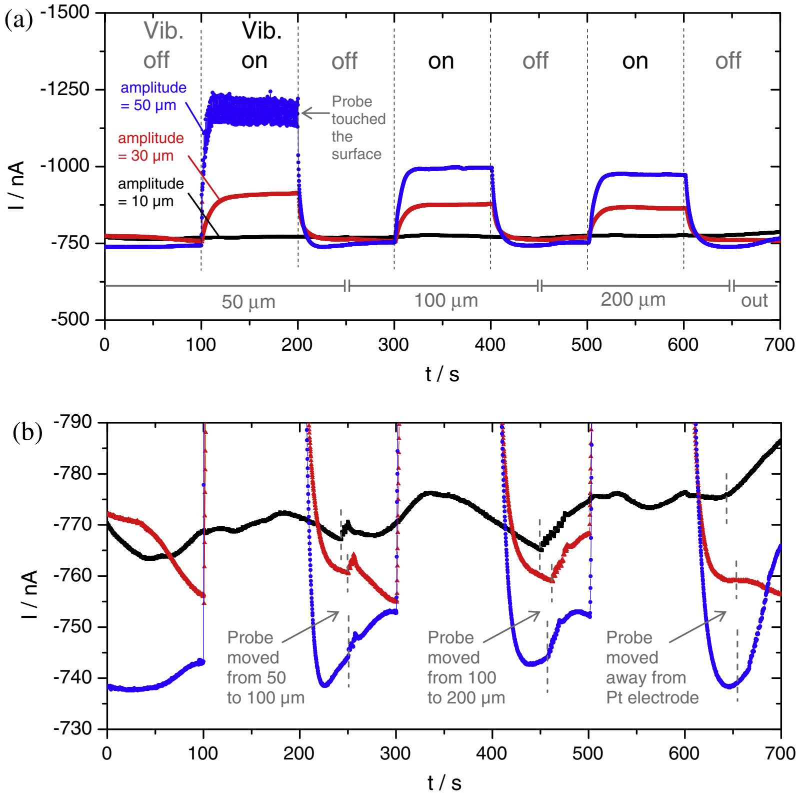

**Fig. 3.** (a) Chronoamperometric currents recorded at −0.75 $V_{Ag|AgCl}$ with the SVET probe placed in the centre of the Pt disk at 50, 100 or 200 μm above the surface, with vibration on or off and different amplitudes (20, 60 and 100 μm peak-to-peak). (b) same as (a) with a different current scale.

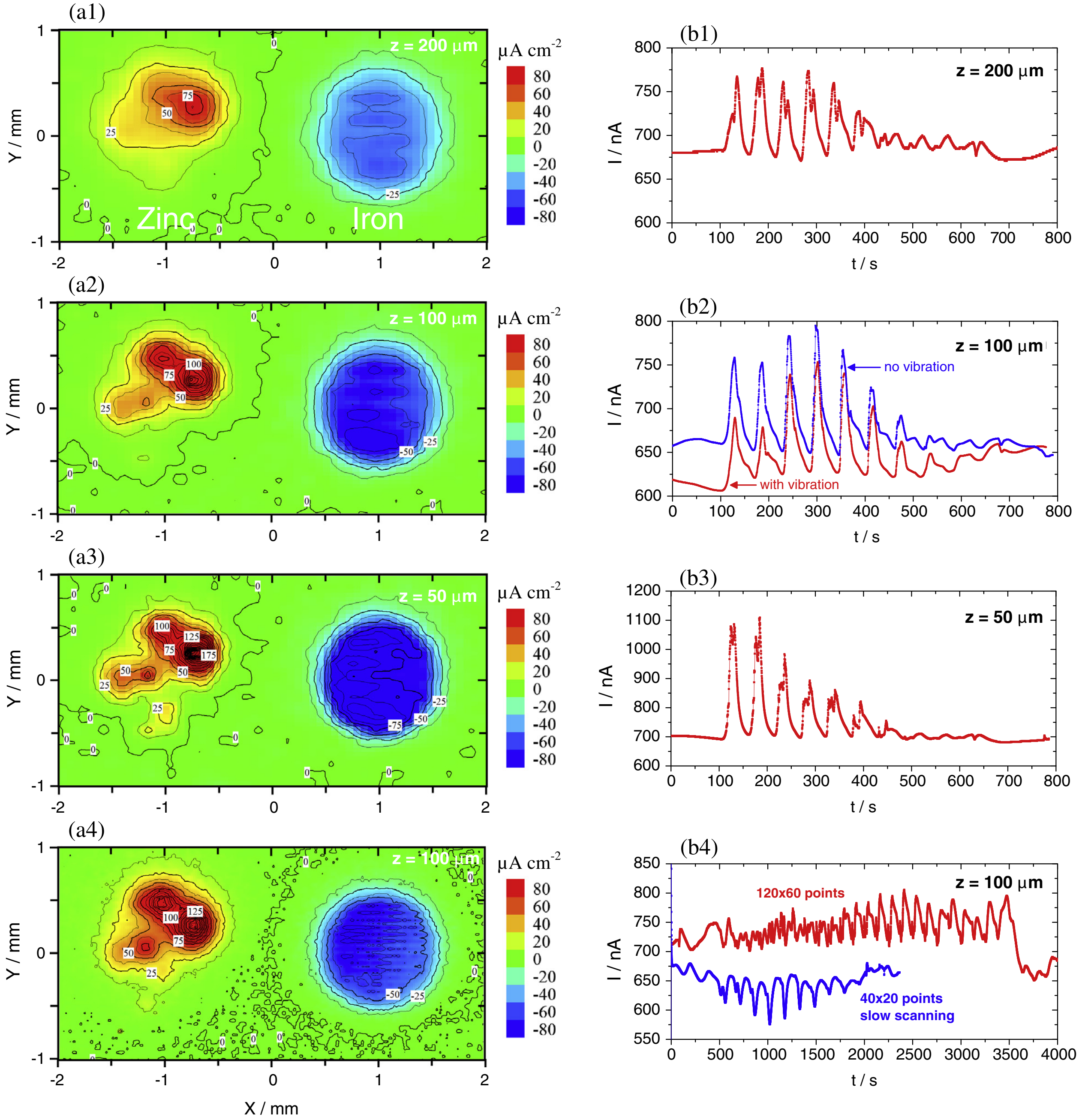

**Fig. 4.** SVET maps (40 × 20 points) (ax) and galvanic current of the Zn–Fe couple (bx) measured in different experimental conditions, as indicated in the graphs. The recording of the galvanic current started when it became stable and the maps started 100 s later.

measurements might have other causes: the probe measures in a plane above the surface, missing the current that flows below and the maps give only the *z* component of the current, omitting the remainder components.

In order to reduce the probe influence, two approaches were experimented with no success (Fig. 4(b4)): slower probe movement between points (70 µm $s^{-1}$ instead of 342 µm $s^{-1}$) and maps with a larger number of points (7200 in place of 800), which means smaller excursions between points. Interestingly, the current pattern was different suggesting a change in the hydrodynamics induced by the probe.

This work analysed SVET operation in its normal operation conditions (probe tip size of 10–20 µm, vibration amplitude of 10 µm and distance-to-sample in the 50–200 µm range).

It is evident that the effect of vibration is not important in normal operation. Conversely, the movement of the probe during scanning does indeed affect the process. It became also clear that the effect of the probe movement should occur with any probe, being it SVET, SRET (scanning reference electrode technique), SECM (scanning electrochemical microscopy) or other. This is a convection effect provoked by the movement of any probe above the sample. It is more important for corrosion systems that are controlled by mass transport, generally the reduction of oxygen.

According to the results obtained in this work, an overestimation of the cathodic current of 10–30% is to be expected in normal conditions. The total corrosion of the sample will not be affected because the effect only lasts while SVET is scanning, rapidly vanishing afterwards. The worst situation would happen if maps were obtained uninterruptedly for a long period of time. But even in this case the increase of the overall corrosion would be 10–30%, according to the present results.

Only the typical conditions of operation were of concern here. Future work is needed to examine the impact of several parameters: probe size, frequency and amplitude of vibration, probe-to-source distance and scanning speed. Experimental characterisation and theoretical modelling are necessary to fully understand the effect of each parameter and the limits of operation in order to prevent or minimize their influence.

## 4. Conclusions

This work analysed the influence of vibration and probe movement during scanning on the SVET results. The analysis focused only on the most typical conditions of SVET operation (probe tip size of 10–20 μm, vibration amplitude of 10 μm and distance-to-sample in the 50–200 μm range). The following conclusions can be drawn for the normal operation of SVET:

1. The vibration of the probe influences the $O_2$ reduction current but the effect is small (5% or less);
2. The influence of vibration increases for larger amplitudes and smaller probe-to-sample distances (but values different from the tested ones are seldom used);
3. The movement of the probe is much more important, leading to an increase in the current up to 10–30% when the probe is passing above the cathodic regions;
4. The SVET probe affects mainly the region below it and the effect vanishes within minutes;
5. The maps are not affected in a perceptible way by SVET operation and, unless the scanning is permanent, it will not affect the corrosion of the sample in the long run;
6. The convection induced by the probe movement seems to be a problem inherent to any scanning probe in solution close to the samples;
7. The effect is more important for systems controlled by mass transport.

## Acknowledgements

M.C. Quevedo thanks CONACYT (Mexico) for the post-doc scholarship approach n° 203529 and A.C. Bastos thanks a post-doc grant with the reference BPD/UI50/2739/2013. Funds from the Research Fund for Coal and Steel (European Commission) project AtCorAS 2011-CT-2011-00015 and Fundação para a Ciência e a Tecnologia (Portugal) project PTDC/CTM-MAT/1515/2012 are also acknowledged

## References

[1] H.S. Isaacs, The measurement of the galvanic corrosion of soldered copper using the scanning vibrating electrode technique, Corros. Sci. 28 (1988) 547–558.
[2] A.J. Aldykiewicz Jr., H.S. Isaacs, Dissolution characteristics of duplex stainless steels in acidic environments, Corros. Sci. 40 (1998) 1627–1646.
[3] K. Ogle, V. Baudu, L. Garrigues, X. Philippe, Localized electrochemical methods applied to cut edge corrosion, J. Electrochem. Soc. 147 (2000) 3654–3660.
[4] B. Vuillemin, X. Philippe, R. Oltra, V. Vignal, L. Coudreuse, L.C. Dufour, E. Finot, SVET, AFM and AES study of pitting corrosion initiated on MnS inclusions by microinjection, Corros. Sci. 45 (2003) 1143–1159.
[5] D. Battocchi, J. He, G.P. Bierwagen, D.E. Tallman, Emulation and study of the corrosion behaviour of Al alloy 2024–T3 using a wire beam electrode (WBE) in conjunction with scanning vibrating electrode technique (SVET), Corros. Sci. 47 (2005) 1165–1176.
[6] A.M. Simões, A.C. Bastos, M.G. Ferreira, Y. González-García, S. González, R.M. Souto, Use of SVET and SECM to study the galvanic corrosion of an iron – zinc cell, Corros. Sci. 49 (2007) 726–739.
[7] F. Thebault, B. Vuillemin, R. Oltra, K. Ogle, C. Allely, Investigation of self-healing mechanism on galvanized steels cut edges by coupling SVET and numerical modeling, Electrochim. Acta 53 (2008) 5226–5234.
[8] G. Williams, A.J. Coleman, H.N. McMurray, Inhibition of aluminium alloy AA2024-T3 pitting corrosion by copper complexing compounds, Electrochim. Acta 55 (2010) 5947–5958.
[9] A.C. Bastos, O.V. Karavai, M.L. Zheludkevich, K.A. Yasakau, M.G.S. Ferreira, Localised measurements of pH and dissolved oxygen as complements to SVET in the investigation of corrosion at defects in coated aluminum alloy, Electroanalysis 22 (2010) 2009–2016.
[10] A.C. Bastos, M.G. Taryba, O.V. Karavai, M.L. Zheludkevich, S.V. Lamaka, M.G.S. Ferreira, Micropotentiometric mapping of local distributions of $Zn^{2+}$ relevant to corrosion studies, Electrochem. Commun. 12 (2010) 394–397.
[11] S. Kallip, A.C. Bastos, M.L. Zheludkevich, M.G.S. Ferreira, A multi-electrode cell for high-throughput SVET screening of corrosion inhibitors, Corros. Sci. 52 (2010) 3146–3149.
[12] J. Ferrier, W.J. Lucas, Ion transport and the vibrating probe, Biophysical J. 49 (1986) 803–807.
[13] H.N. McMurray, D. Williams, D.A. Worsley, Artifacts induced by large-amplitude probe vibrations in localized corrosion measured by SVET, J. Electrochem. Soc. 150 (2003) B567–B573.
[14] A.C. Bastos, A.M. Simões, M.G. Ferreira, Corrosion of electrogalvanized steel in 0.1M NaCl studied by SVET, Port. Electrochim. Acta 21 (2003) 371–387.
[15] C. Scheffey, Electric fields and the vibrating probe, for the uninitiated, in: R. Nucitelli (Ed.), Ionic Currents in Development, Alan R. Liss Inc., New York, 1986, pp. xxv–xxxvii.
[16] C. Scheffey, Two approaches to construction of vibrating probes for electric current measurement in solution, Rev. Sci. Instrum. 59 (1988) 787–792.
[17] H.S. Isaacs, The effect of height on the current distribution measured with a vibrating electrode probe, J. Electrochem. Soc. 138 (1991) 722–728.
[18] L. Nanis, W. Kesselman, Engineering applications of current and potential distributions in disk electrode systems, J. Electrochem. Soc. 118 (1971) 454–461.
[19] R. Venkatesan, Study of corrosion product of zinc in natural sea water, Brit. Corros. J. 33 (1998) 77–80.